Immunity, Vol. 16, 193–204, February, 2002, Copyright ©2002 by Cell Press

WIP Deficiency Reveals a Differential Role for WIP and the Actin Cytoskeleton in T and B Cell Activation

Inés M. Antón,[1,5,6] Miguel A. de la Fuente,[1,5] Tasha N. Sims,[2] Sheryl Freeman,[1] Narayanaswamy Ramesh,[1] John H. Hartwig,[3] Michael L. Dustin,[2] and Raif S. Geha[1,4]
[1]Division of Immunology
Children's Hospital and Department of Pediatrics
Harvard Medical School
Boston, Massachusetts 02115
[2]Skirball Institute of Biomolecular Medicine
New York University School of Medicine
New York, New York 10016
[3]Division of Experimental Medicine
Brigham and Women's Hospital and
Harvard Medical School
Boston, Massachusetts 02115

Summary

WIP stabilizes actin filaments and is important for filopodium formation. To define the role of WIP in immunity, we generated WIP-deficient mice. WIP$^{-/-}$ mice have normal lymphocyte development, but their T cells fail to proliferate, secrete IL-2, increase their F-actin content, polarize and extend protrusions following T cell receptor ligation, and are deficient in conjugate formation with superantigen-presenting B cells and anti-CD3 bilayers. In contrast, WIP-deficient B lymphocytes have enhanced proliferation and CD69 expression following B cell receptor ligation and mount normal antibody responses to T-independent antigens. Both WIP-deficient T and B cells show a profound defect in their subcortical actin filament networks. These results suggest that WIP is important for immunologic synapse formation and T cell activation.

Introduction

The actin cytoskeleton is emerging as an integral component in T lymphocyte activation following the interaction between the T cell receptor (TCR) and peptide-loaded major histocompatibility complex (MHC) molecules on the surface of antigen-presenting cells (APCs) (Dustin and Cooper, 2000; Penninger and Crabtree, 1999). Interaction between T lymphocytes and APCs induces the formation of molecular clusters at the contact site that are enriched in polymerized filamentous actin (F-actin) (Grakoui et al., 1999; Monks et al., 1998). These supramolecular activation clusters (SMACs), also named immunological synapses, contain several signaling components. They include TCR/CD3, src and Syk family kinases, and adaptor proteins such as SLP-76, Fyb, and Nck that are linked directly or indirectly to proteins that are involved in actin polymerization, such as Wiskott Aldrich Syndrome protein (WASP) and Ena/VASP family members (Grakoui et al., 1999; Krause et al., 2000; Monks et al., 1998). The accumulation of F-actin at the T cell-APC interface is thought to stabilize a continuous contact between T cells and APCs, which is required for optimal T cell activation. Inhibition of actin polymerization by cytochalasin blocks formation of the immunological synapse and T cell activation (Holsinger et al., 1998; Wulfing et al., 1998).

Wiskott Aldrich Syndrome (WAS) is a severe X-linked immunodeficiency caused by mutations in the *WASP* gene (Derry et al., 1994). WASP is the first identified member of an expanding family of proteins involved in signaling and cytoskeletal organization that include N-WASP and Scar/WAVE (Machesky and Insall, 1998; Miki et al., 1996, 1998a). TCR signaling results in the activation of Vav, which is an exchange factor for the small GTPase Cdc42. GTP-loaded Cdc42 binds to WASP (Aspenstrom et al., 1996; Kolluri et al., 1996; Symons et al., 1996) and its homolog N-WASP (Miki et al., 1998b), causing a conformational change that allows them to interact with the Arp2/3 complex and initiate actin polymerization (Kim et al., 2000; Miki et al., 1996; Rohatgi et al., 2000). WASP plays a critical role in T cell activation and in the reorganization of the actin cytoskeleton that follow TCR engagement. This is evidenced by the markedly impaired proliferation of T cells from WAS patients and WASP-deficient mice to anti-CD3 mAb and by their decreased ability to form caps and to increase their F-actin content following TCR/CD3 ligation (Gallego et al., 1997; Molina et al., 1993; Snapper et al., 1998; Zhang et al., 1999).

The WASP-interacting protein (WIP) is a proline-rich 503 aa long protein that shows homology in its N-terminal end to the yeast polarity development protein verprolin (Ramesh et al., 1997). Several lines of evidence point to the importance of WIP in regulating the actin cytoskeleton. First, WIP interacts with G-actin, F-actin, and with the actin polymerization regulating protein profilin (Martinez-Quiles et al., 2001; Ramesh et al., 1997). Second, introduction of human WIP into verprolin-deficient yeast corrects their cell growth, cytoskeletal organization, endocytosis, and cell polarity defects (Vaduva et al., 1999). Third, WIP overexpression in human B cell lines causes an increase in cellular F-actin content and induces the formation of subcortical patches of actin (Ramesh et al., 1997). Fourth, WIP regulates N-WASP-induced actin nucleation (Martinez-Quiles et al., 2001). Finally, WIP is important for filopodium formation (Martinez-Quiles et al., 2001) and for actin tail generation by vaccinia virus (Moreau et al., 2000). To investigate the role of WIP in TCR-mediated T cell activation and cytoskeletal organization, we generated WIP null mice by gene targeting.

Results

Generation of WIP-Deficient Mice

A targeting construct in which coding exons two to five of the murine *wip* gene were replaced with a neomycin-resistant gene was introduced in ES cells (Figure 1A). ES clones with targeted disruption of one *wip* allele were

[4]Correspondence: raif.geha@tch.harvard.edu
[5]These authors contributed equally to this work.
[6]Present address: Dipartimento di Scienze Cliniche e Biologiche, Ospedale San Luigi Gonzaga, 10043 Orbassano, Italy.

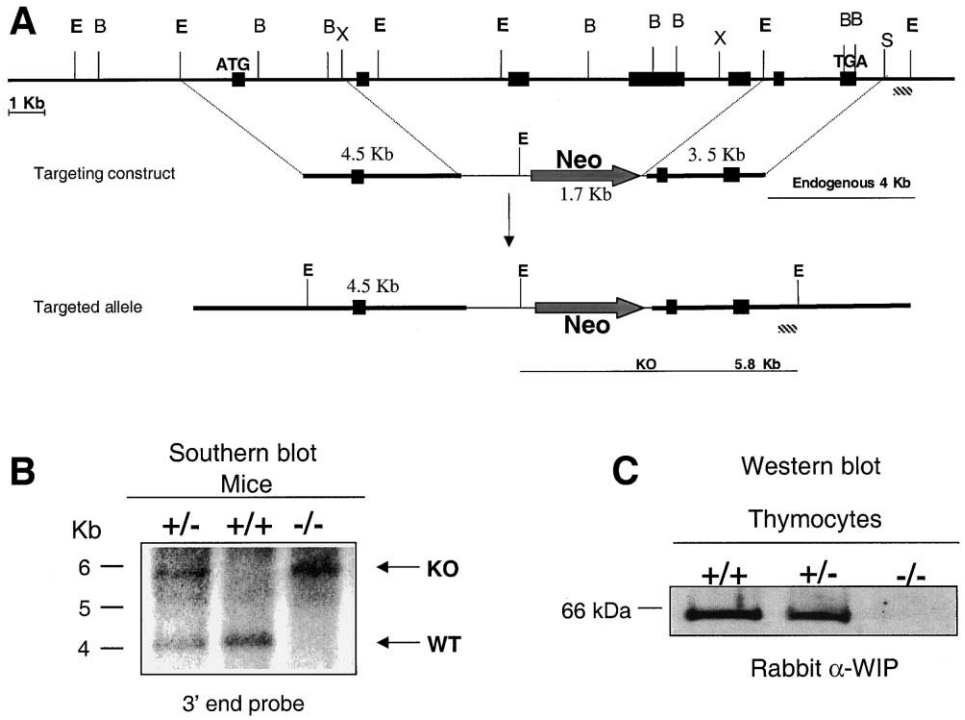

Figure 1. Generation of WIP-Deficient Mice

(A) Genomic structure of the *wip* gene and predicted structure of the targeted allele after homologous recombination. Exons are represented by black boxes. Neo, neomycin resistance gene. The 650 bp SacI/EcoRI hybridization probe is shown as a patterned box. B, BamHI; E, EcoRI; S, SacI; and X, XbaI (not all restriction sites are shown).

(B) Southern blot analysis of tail DNA. Genomic DNA was digested by EcoRI and probed with the 650 bp fragment immediately 3′ to the targeted locus, shown in (A). The WT allele is represented by the 4 kb band. The knockout allele is represented by the 5.8 kb band.

(C) Western blot analysis of WIP from thymocytes using rabbit antibody against an ESRSGSNRRERGAP WIP peptide.

identified in Southern blots by the presence of a novel 5.8 kb fragment derived from the targeted allele in addition to the 4 kb fragment derived from the WT allele. Of 97 ES clones analyzed, one was found to have a disrupted allele and was used to generate WIP$^{-/-}$ mice, which were identified by Southern blot analysis (Figure 1B). Western blot analysis of lysates from thymocytes, lymph nodes (LN), and splenocytes confirmed the absence of WIP expression in WIP$^{-/-}$ mice (Figure 1C and data not shown). WIP$^{-/-}$ mice did not display apparent differences from WT littermates in growth, weight, or health.

Normal Lymphoid Development in WIP-Deficient Mice

Thymus cellularity in WIP$^{-/-}$ mice 6–10 weeks of age was significantly reduced compared to WT littermates ($106 \pm 66 \times 10^6$ cells in KO versus $220 \pm 94 \times 10^6$ cells in WT, $n = 6$, $p = 0.03$). Detailed FACS analysis of thymocytes at 6–10 weeks of age revealed no obvious differences in the percentages of CD4$^+$ and CD8$^+$ cells, or of CD3, TCR$\alpha\beta$, TCR$\gamma\delta$, and CD2 positive cells (data not shown). There were no obvious differences between spleen and LN from 6- to 8-week-old WIP$^{-/-}$ and WT littermates as to numbers or percentages of CD4$^+$, CD8$^+$, B220$^+$, IgM$^+$, IgD$^+$, and Thy1$^+$ cells (data not shown). Bone marrow cells from the same WIP$^{-/-}$ mice had a normal profile of staining for B220, IgM, and CD43, and the numbers of B220$^+$, CD5$^+$ B1 cells in the peritoneum of WIP$^{-/-}$ mice were normal (data not shown). These results suggest that WIP is not essential for the development of B and T lymphocytes.

Increased Proliferation and IL-2 Receptor Expression in B Cells from WIP$^{-/-}$ Mice in Response to Stimulation

Pure B cells (>80% B220$^+$) from WIP$^{-/-}$ mice showed markedly increased proliferation in response to anti-IgM, lipopolysaccharide (LPS), and anti-CD40 mAb with or without IL-4 (Figure 2A). Activated B cells express increased levels of CD69 (Risso et al., 1989). There was increased expression of CD69 on B cells from WIP$^{-/-}$ mice following stimulation with LPS, anti-CD40, LPS+IL-4, and anti-CD40+IL-4 compared to B cells from WT littermates (Figure 2B and data not shown). The enhanced response of WIP$^{-/-}$ B cells to BCR ligation was not simply due to failure of internalization of the BCR, which terminates signaling, because they internalized their BCR normally following anti-IgM crosslinking, as assessed by FACS (data not shown).

BCR ligation results in tyrosine phosphorylation of several proteins (reviewed in Benschop and Cambier, 1999 and Kurosaki et al., 2000). Following anti-IgM stimulation, tyrosine phosphorylation of proteins <50 kDa in mol wt was enhanced in WIP$^{-/-}$ B cells (Figure 2C).

Serum Immunoglobulins and Antibody Responses in WIP$^{-/-}$ Mice

Serum IgM and IgE levels were significantly elevated in 6- to 8-week-old WIP$^{-/-}$ mice compared to WT littermates, while serum IgG subclasses and serum IgA were not significantly different (Figure 3A).

To determine the role of WIP in antibody immune

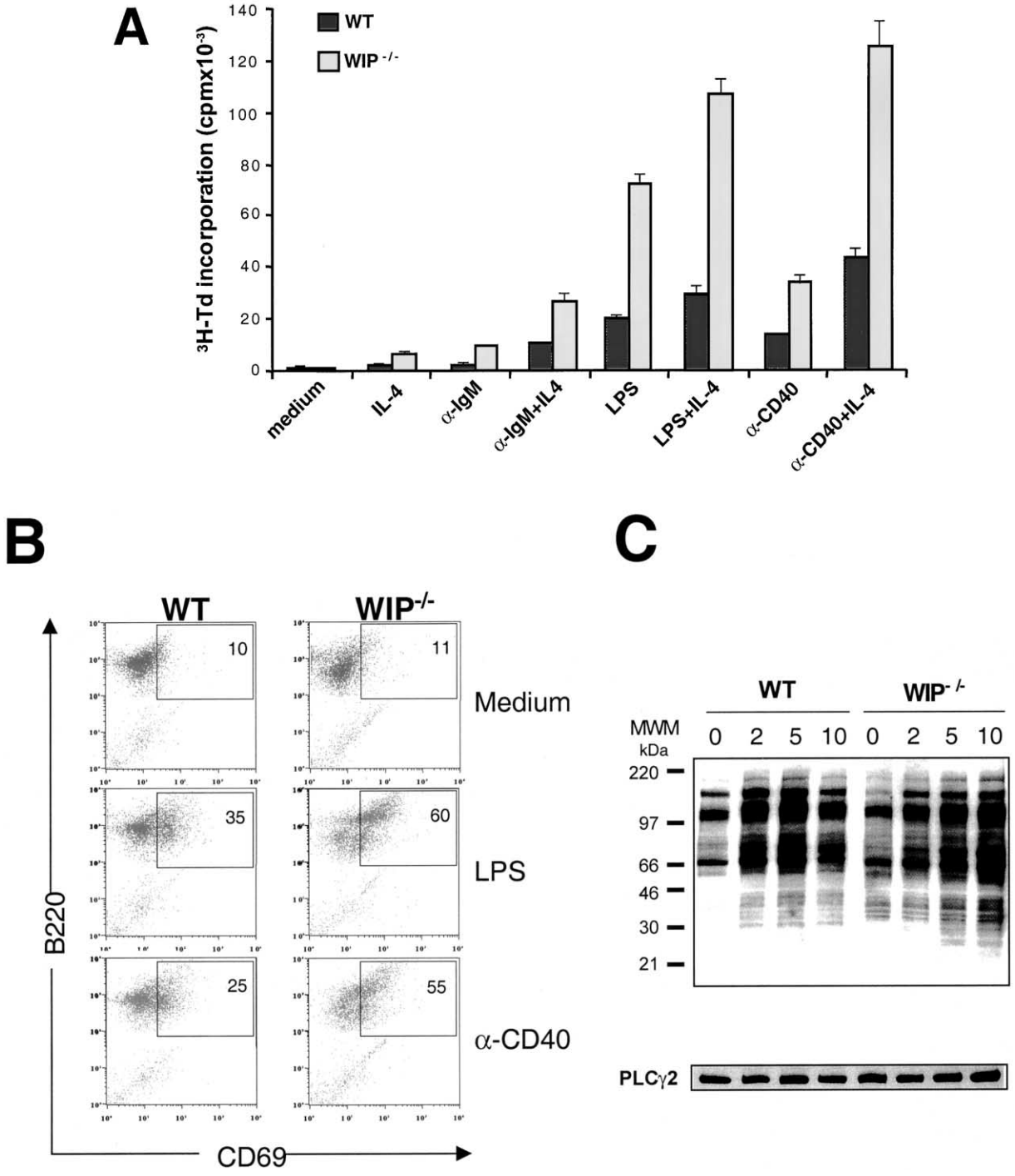

Figure 2. B Cell Activation in WIP$^{-/-}$ Mice

(A) Proliferation: Purified spleen B cells from 6- to 9-week-old mice were cultured in medium alone or in the presence of stimuli, and proliferation was measured by [^{3}H]-thymidine incorporation. Error bars represent SDs of triplicate values. Similar results were obtained in four experiments.
(B) Activation markers: Splenic B cells from 6- to 9-week-old mice were incubated for 20 hr with the indicated stimuli and then analyzed by FACS for expression of CD69 and B220. Similar results were obtained in two other experiments.
(C) Protein tyrosine phosphorylation: Splenic B cells from 6- to 9-week-old mice were incubated at 37°C for the indicated times (min) with anti-IgM, lysed, run on SDS-PAGE, transferred to nitrocellulose, and developed with anti-phosphotyrosine antibody. The membrane was stripped and reprobed with anti-PLCγ2 as a loading control. Identical results were obtained in two other experiments.

responses, we immunized WT, WIP$^{-/-}$ mice and WIP$^{+/-}$ littermates with the T-dependent (TD) antigen TNP-KLH and T-independent (TI) antigens. WIP$^{+/-}$ mice had serum immunoglobulins and antibody responses indistinguishable from those of WT controls (data not shown). WIP$^{-/-}$ mice had normal or slightly increased IgM antibody responses but virtually undetectable IgG responses to both KLH (Figure 3B) and TNP (data not shown). Both

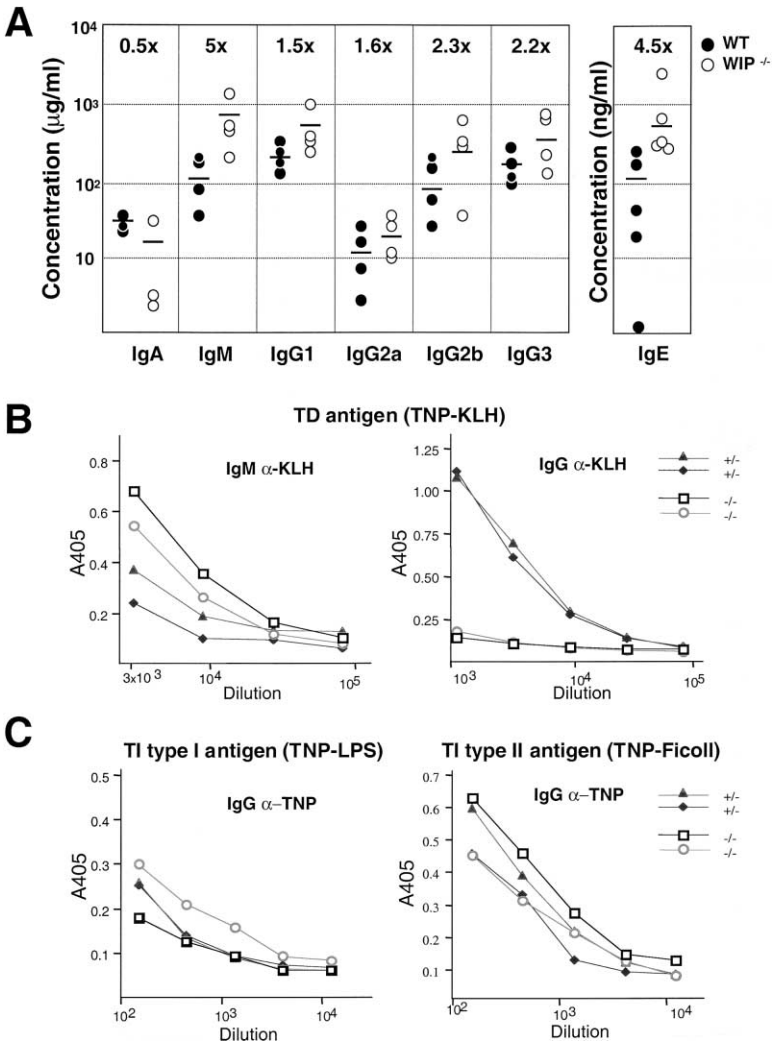

Figure 3. Antibody Production in WIP$^{-/-}$ Mice

(A) Serum immunoglobulin levels from nonimmunized 6- to 8-week-old WIP$^{-/-}$ (open circles) mice and WT littermates (filled circles) as determined by isotype-specific ELISA.

(B) IgM and IgG antigen-specific antibody responses of 12- to 15-week-old mice to KLH following immunization with the TD antigen TNP-KLH as determined by ELISA.

(C) IgG antigen-specific antibody responses of 12- to 15-week-old mice to TNP following immunization with the TI type I (TNP-LPS) or TI type II (TNP-Ficoll) antigens as determined by ELISA.

IgG and IgM antibody responses of WIP$^{-/-}$ mice to the type I TI antigen TNP-LPS and to the type II TI antigen TNP-Ficoll were normal (Figure 3C and data not shown).

WIP Is Essential for T Cell Activation via the TCR/CD3 Complex

Proliferation in response to plate-bound anti-CD3 was abolished in WIP$^{-/-}$ T lymphocytes at all coating concentrations tested (Figure 4A). In contrast, proliferation to PMA + ionomycin, which bypasses receptor signaling, was normal.

Interactions between IL-2 and IL-2 R play an important role in T cell proliferation, and optimal production of IL-2 by T cells requires costimulation via CD28 (Rudd, 1996). The failure of WIP$^{-/-}$ T cells to proliferate to anti-CD3 was corrected by addition of IL-2 but not by costimulation with anti-CD28 mAb (Figure 4B). WIP$^{-/-}$ T cells poorly upregulated IL-2Rα chain expression following anti-CD3 stimulation (Figure 4C). This was only modestly enhanced by costimulation with anti-CD28 and almost completely corrected by addition of IL-2. Similar results were obtained for CD69 expression (data not shown). WIP$^{-/-}$ T cells failed to secrete detectable IL-2 after CD3 ligation even upon costimulation with anti-CD28 as determined by bioassay (Figure 4D) and ELISA (data not shown).

TCR/CD3 ligation causes rapid activation of a number of tyrosine kinases, resulting in tyrosine phosphorylation of several proteins that play important roles in TCR signal transduction (reviewed in Acuto and Cantrell, 2000). Following anti-CD3 stimulation, protein tyrosine phosphorylation was grossly intact in WIP$^{-/-}$ T cells (data not shown), and calcium fluxes were only slightly decreased (~15% decrease, n = 4 experiments). Erk phosphorylation was also slightly decreased, whereas JNK phosphorylation was normal (Figure 4E). Furthermore, there was no detectable impairment in the nuclear translocation of NFκB and NFATc as assessed by immunofluorescence (data not shown).

WIP$^{-/-}$ T Cells Do Not Increase F-Actin Content or Form Protrusions and Pseudopodia following TCR/CD3 Ligation

TCR/CD3 ligation causes an increase in the cellular F-actin of normal T cells (Phatak and Packman, 1994). The effect of TCR/CD3 ligation on cellular F-actin content was examined by staining permeabilized cells with TRITC-labeled

phalloidin. In four experiments, the amount of F-actin in unstimulated WT and WIP$^{-/-}$ T cells was similar (data not shown). However, in contrast to T cells from WT littermates, T cells from WIP$^{-/-}$ mice failed to increase their F-actin content following stimulation with anti-CD3 (Figure 5A).

Engagement of the TCR/CD3 complex triggers a distinct pattern of reorganization of cellular F-actin (Bunnell et al., 2001; Parsey and Lewis, 1993). Cytoskeletal reorganization was examined in T cells activated using coverslip-bound anti-CD3 antibody. This system closely mimics T cell activation by MHC class II-peptide complexes arrayed on the surface of APCs by creating a polarized stimulus that induces T cells to undergo the morphological changes necessary to maximize the contact between their antigen receptors and the activating surface (Bunnell et al., 2001). Unstimulated T cells from WT and WIP$^{-/-}$ mice exhibited a similar staining pattern with prominent actin rings, as previously described (Parsey and Lewis, 1993). After incubation for 20 min over anti-CD3 coated glass coverslips, T cells from WT mice acquired a polarized shape, had less prominent actin rings, and spread by making microspikes and blunt pseudopodia enriched in F-actin (Figure 5B and video frames in Figure 5C). The surface projections were visualized by fluorescence microscopy, although they were difficult to detect by differential interference contrast used in the time lapse videomicroscopy. In contrast, T cells from WIP$^{-/-}$ mice maintained a round shape with persistence of a strong actin ring. More importantly, they spread very poorly on anti-CD3 coated surface and had markedly reduced ability to make cortical protrusions (Figure 5B and video frames in Figure 5C). However, actin cap formation following stimulation with immobilized anti-CD3 for 20 min was similar in WIP$^{-/-}$ T cells and controls (52% versus 54% capped cells).

The failure of T cells from WIP$^{-/-}$ mice to spread and to develop projections following TCR/CD3 ligation prompted us to examine their dynamics when exposed to an anti-CD3 coated surface. Purified T cells were plated on anti-CD3 coated or anti-B220 coated glass coverslips and observed with videomicroscopy for 20 min. T cells from WT and WIP$^{-/-}$ mice attached to a similar extent to the anti-CD3 coated surface but did not attach to the anti-B220-coated control surface (data not shown). The change in shape and polarized appearance of T cells from WT mice after incubation with bound anti-CD3 for the indicated times from 0–14 min are illustrated in Figure 5C. During the course of the video, 90% of tracked T cells from WT mice cells extended protrusions that later retracted, only to appear again in other areas of the cell. In contrast, T cells from WIP$^{-/-}$ mice did not acquire a polarized shape; only 9% of them exhibited protrusions at some point, and the number and the movement of these protrusions were drastically reduced.

Contact Formation with Anti-CD3 Bilayers and Conjugate Formation with APCs Are Impaired in WIP$^{-/-}$ T Cells

The poor response of WIP$^{-/-}$ T cells to anti-CD3 could be related to defects in TCR clustering. We tested this hypothesis using a planar bilayer substrate in which fluorescently labeled anti-CD3 mAb is laterally mobile and ICAM-1 provides adhesion. Equivalent clustering of anti-CD3 in contacts of WT and WIP$^{-/-}$ T cells was observed by 4 min (data not shown). By 20 min, the WT cells displayed extensive contact areas with the planar bilayer and colocalization of F-actin and GM1 in the contact area (Figure 6A). Total GM1 in WT and WIP$^{-/-}$ cells was similar in level, but the amount of GM1 in the contact areas was greater in WT cells. The mobility of the WT cells on the surface resulted in dispersion of the clustered anti-CD3, but the total amount of clustered anti-CD3 in WT contacts remained the same when integrated over the large contact areas. After 20 min, WIP$^{-/-}$ T cells formed smaller contact areas with lower levels of F-actin and GM1 than WT cells but still contained clustered anti-CD3 mAb (Figure 6A). The difference in contact area was statistically significant (Figure 6B), while the trends in F-actin and GM-1 localization were consistently observed but were not statistically significant upon quantification (data not shown).

The above results suggested that WIP$^{-/-}$ T cells might have defects in forming an immunological synapse upon interaction with APCs. Since WIP$^{-/-}$ mice have not yet been bred on a TCR transgenic background, we employed I-E^{k} positive APC and the superantigen Staphylococcal Enterotoxin A (SEA) to trigger initial stages of synapse formation (Wulfing et al., 2000). An early actin-dependent stage in immunological synapse formation has been identified as an extensive interface between the T cell and APC (Negulescu et al., 1996; Wulfing et al., 1998). Formation of this broad interface with pseudopod extension is most prominent at 2 min and is actin dependent. WT cells formed a classical extended interface in which clustering of the integrin LFA-1 was observed (Figure 6Ca and 6Cc). The extension of pseudopodia resulted in a contact angle greater than 90° with the APC in all WT cells conjugates observed (Figure 6Ca). At this time, TCR redistribution was not detectable (Figure 6Cb), although SEA was required to observe conjugates providing evidence of TCR-SEA-MHC interactions. WIP$^{-/-}$ T cells displayed 2-fold fewer conjugates (data not shown) and a significantly smaller interface both at the 2 and 5 min time points (Figure 6D). The contact angle was also always smaller than 90° indicating that the WIP$^{-/-}$ T cells remained round, a situation that was never observed with WT cells at that time. Despite the overall defect in contact formation, LFA-1 was still accumulated to a similar extent as in the WT T cell conjugates.

The cortical actin network is disrupted in WIP-deficient lymphocytes. WIP stabilizes actin filaments (Ramesh et al., 1997). This prompted us to examine the architecture of the actin network in WIP$^{-/-}$ lymphocytes. Purified T and B cells were adhered to anti-CD3 and anti-IgM coated coverslips, respectively, and their actin network was directly visualized by electron microscopy by unroofing pseudopods to reveal the basal cell membrane. The cytoplasmic surface of the plasma membrane of adherent unstimulated WT T cells was decorated with a loose network of F-actin (Figure 7A, upper left panel). Activation over anti-CD3 coated coverslips for 15 min led to recruitment of additional F-actin (Figure 7A, bottom left panel) and formation of prominent protrusions (Figure 7A, inset in bottom left panel). In marked

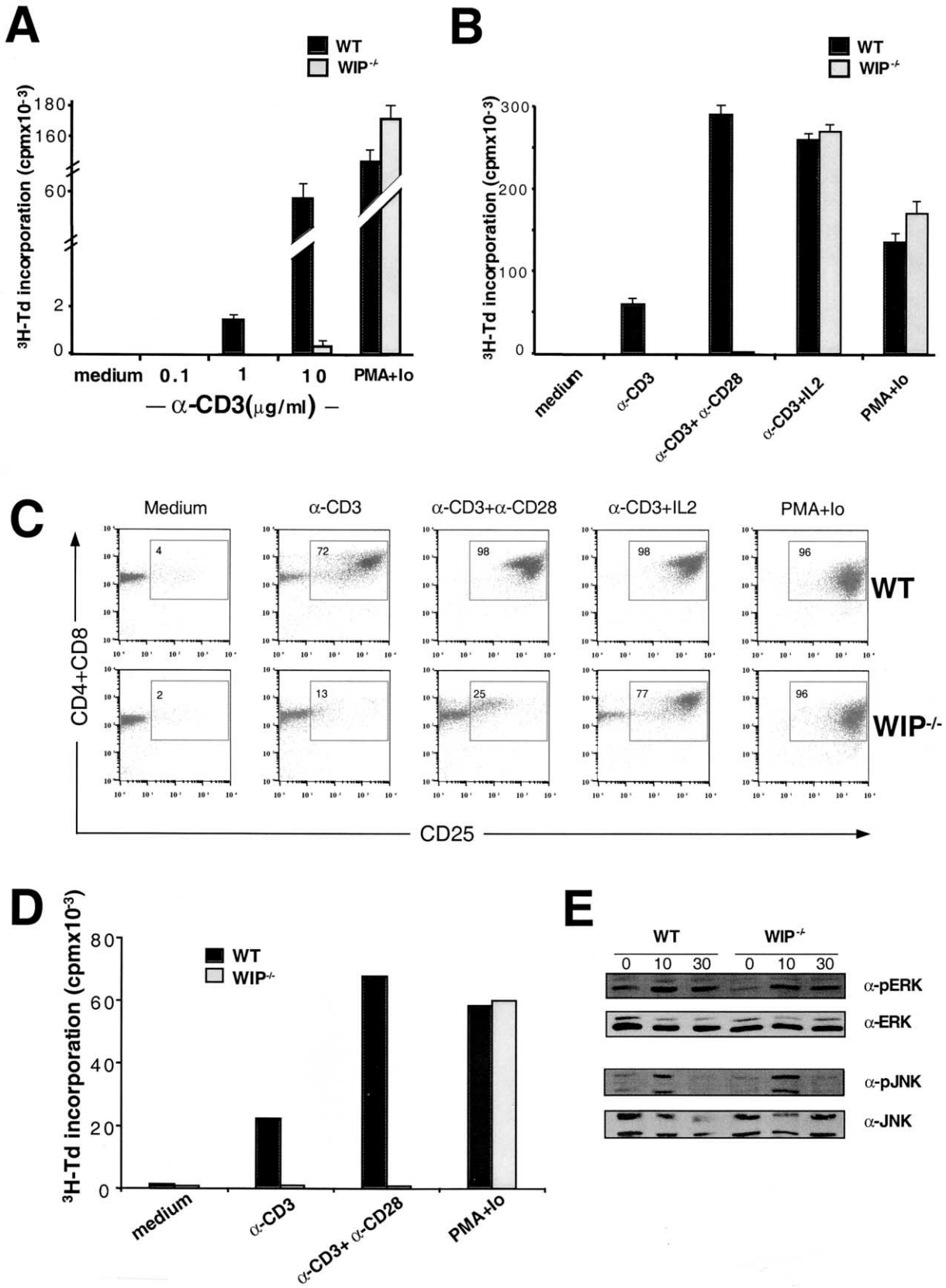

Figure 4. Antigen Receptor-Induced Proliferation and Activation in Purified T WIP$^{-/-}$ T Cells

(A) Purified LN T cells from 6- to 10-week-old WT mice and WIP$^{-/-}$ littermates were stimulated in wells coated with increasing concentrations of anti-CD3ε or in the presence of PMA and ionomycin. T cells were cultured for 48 hr, pulsed with 1 μCi [^{3}H]-thymidine for an additional 16 hr, then

contrast, although the total basal F-actin content was similar in WT and WIP $^{-/-}$ T cells (Figure 5A), the plasma membrane of adherent WIP$^{-/-}$ T cells was sparsely coated with F-actin, and activation did little to alter this coating (Figure 7A, upper and bottom right panels), resulting in less prominent protrusions than in WIP$^{+/-}$ cells (Figure 7A, inset in bottom right panel). These findings suggest that WIP is essential for the integrity of the actin cytoskeleton in T cells and for its reorganization following TCR engagement.

A similar defect in the actin network was also found in WIP-deficient B cells. The cytoplasmic surface of the plasma membrane of B cells from WIP$^{+/-}$ mice was decorated with a loose network of F-actin (Figure 7B, upper left panel), and there was no increase in the density of the actin network following anti-IgM stimulation (Figure 7B, bottom left panel). This was consistent with the observation that anti-IgM stimulation caused a marginal increase in F-actin content of B cells (data not shown). The plasma membrane of adherent WIP$^{-/-}$ B cells is sparsely coated with F-actin (Figure 7B, upper right panel) and, like the others, was not changed following anti-IgM stimulation (Figure 7B, bottom right panel). These findings suggest that WIP is also important for the integrity of the actin cytoskeleton in B cells.

Discussion

Our results indicate that WIP is critical for the integrity of the actin cytoskeleton in both T and B lymphocytes and is essential for T cell, but not B cell, activation.

Although WIP is widely expressed, WIP$^{-/-}$ mice appear normal and show no gross abnormalities. Moreover, except for a modest reduction in thymocyte numbers in WIP$^{-/-}$ mice, WIP is dispensable for T and B lymphocyte development but is essential for T cell activation and proliferation in response to ligation of the TCR/CD3 complex. T cells from WIP$^{-/-}$ mice completely failed to proliferate and secrete IL-2 in response to anti-CD3 (Figure 4). Correction of the proliferation defect and upregulation of CD25 expression by anti-CD3 suggest residual CD3 signaling in WIP$^{-/-}$ T cells. The failure of anti-CD28 costimulation to correct the proliferative defect of WIP$^{-/-}$ T cells may reflect a requirement for a higher threshold of signaling via CD3 and/or a requirement for WIP in CD28 signaling. CD28 may be linked to WIP by Vav (Klasen et al., 1998), which synergizes with WIP in inducing NFAT activity and IL-2 production (Savoy et al., 2000).

Failure of WIP$^{-/-}$ mice to undergo IgG isotype switching in vivo following immunization with the TD antigen TNP-KLH (Figure 3B) reflects deficient T cell help rather than an intrinsic abnormality in the B cells since IgG isotype switching in response to type I and type II TI antigens was normal (Figure 3C).

WIP was not essential for the early biochemical events that follow TCR engagement since calcium mobilization and total protein tyrosine phosphorylation, JNK phosphorylation, and nuclear translocation of NFκB and NFAT were all essentially normal in WIP$^{-/-}$ T cells. However, T cells from WIP$^{-/-}$ mice failed to increase their F-actin content following TCR/CD3 ligation (Figure 5A). Inhibition of actin polymerization with cytochalasin D blocks both calcium flux and IL-2 secretion induced by crosslinking of the TCR/CD3 complex (Valitutti et al., 1995). Furthermore, TCR ligation induces association of tyrosine-phosphorylated CD3ζ with the actin cytoskeleton. Disruption of this association results in reduced IL-2 production but preserved tyrosine phosphorylation (Rozdzial et al., 1995). The failure of T cells from WIP$^{-/-}$ mice to secrete IL-2 is consistent with their failure to increase F-actin content. The well-preserved calcium flux in these cells could be explained by a less stringent requirement for actin polymerization and by residual actin polymerization activity in WIP$^{-/-}$ T cells, compared to its complete inhibition caused by cytochalasin D.

Activation of Jurkat T cells with immobilized anti-CD3 antibodies provokes a distinctive pattern of F-actin reorganization and characteristic changes in cell shape (Bunnell et al., 2001). This includes progressive dissolution of actin rings followed by cellular spreading and formation of pseudopods (Parsey and Lewis, 1993). We found similar results when we stimulated WT murine T cells with coverslip bound anti-CD3 antibody: the actin ring attenuates, actin-rich microspikes appear on the cell surface, and pseudopodia form and attach to the stimulating surface. In contrast, T cells from WIP$^{-/-}$ mice conserve their actin rings and fail to form protrusions and pseudopodia following anti-CD3 stimulation (Figure 5B). This suggests an essential role of WIP in cytoskeletal reorganization after TCR engagement.

Upon initial TCR triggering by engagement with peptide-MHC in the APC surface, T cells polarize toward the APC, crawl around them, and spread lamellipodia. These changes, which require a functional actin cytoskeleton (Valitutti et al., 1995), allow the sustained association of multiple TCR/peptide-MHC complexes required for triggering optimal T cell activation. WIP$^{-/-}$ T cells fail to acquire a polarized shape and exhibit very few motile protrusions when exposed to an anti-CD3 coated

collected and scintillation counted. Error bars represent SDs of triplicate values. Displayed are the results of one experiment representative of the four performed with similar results.

(B) Purified LN T cells from 6- to 10-week-old WT mice and WIP$^{-/-}$ littermates were stimulated in wells coated with 10 μg/ml anti-CD3 in the presence of plate-bound anti-CD28 (10 μg/ml) or soluble IL-2 (40 ng/ml). Experimental conditions are as described in (A). Error bars represent SDs of triplicate values. Displayed are the results of one experiment representative of the three performed with similar results.

(C) FACS analysis of CD25 surface expression on purified CD4$^+$/CD8$^+$T cells from 6- to 10-week-old mice before and after stimulation in wells coated with 10 μg/ml anti-CD3 with or without the addition of plate-bound anti-CD28 (10 μg/ml) or IL-2 (40 ng/ml) for 20 hr.

(D) Purified LN T cells from 6- to 10-week-old WT mice and WIP$^{-/-}$ littermates were stimulated in wells coated with 10 μg/ml anti-CD3 with or without addition of anti-CD28 (10 μg/ml) for 96 hr. Supernatants were then collected and assayed for IL-2 by examining their capacity to induce the proliferation of the IL-2-dependent cell line CTLL2.

(E) Purified LN T cells from 12- to 14-week-old mice were stimulated on anti-CD3+anti-CD28 coated plates for the indicated times. Cell lysates were blotted with anti-phosphoERK and anti-ERK as loading control and with anti-phosphoJNK and anti-JNK as loading control.

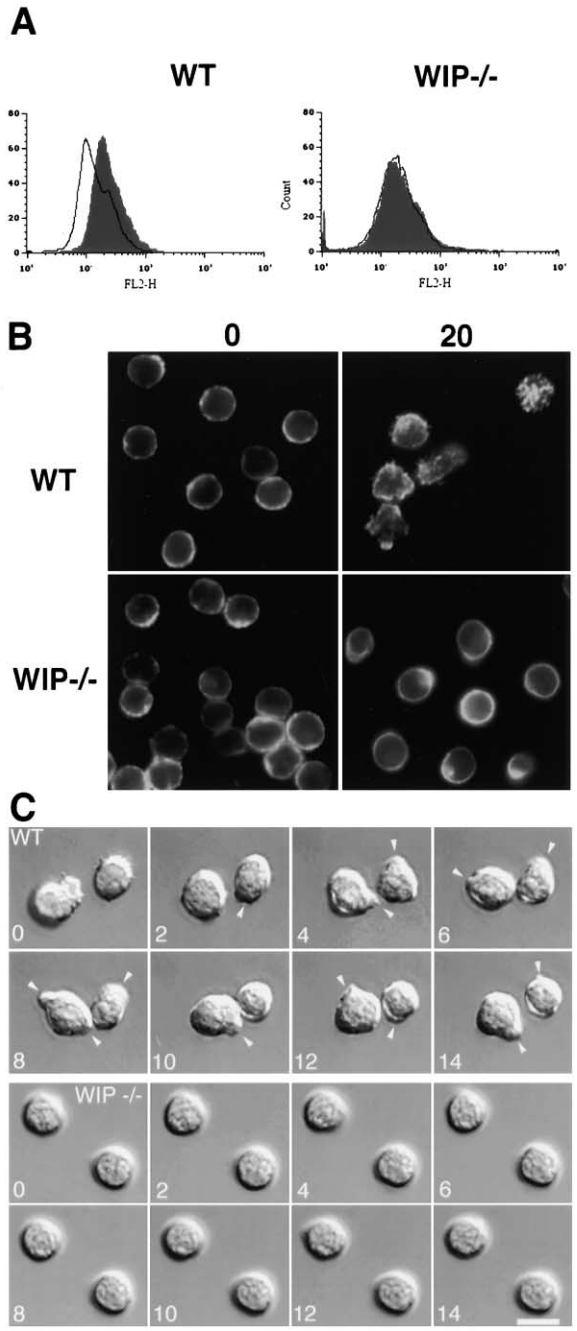

Figure 5. F-Actin Content and Distribution and Time Lapse Videomicroscopy of T Cells after Stimulation with Anti-CD3

(A) Purified LN T cells from 9- to 14-week-old WT or WIP$^{-/-}$ mice were stimulated with anti-CD3 followed by crosslinking with a secondary anti-rat antibody. After 20 min, the cells were fixed, permeabilized, stained with phalloidin-TRITC, and analyzed by FACS. Similar data were obtained in three other experiments.

(B) Purified T lymphocytes were stimulated on anti-CD3 coated glass coverslips. After 20 min, the cells were fixed, stained with phalloidin-TRITC, and examined by fluorescent microscopy.

(C) Purified T cells from WT and WIP$^{-/-}$ mice were added to anti-CD3 coated glass coverslips and allowed to sediment for 30 min at 4°C. After washing off unattached cells, warm (37°C) medium was added, and the cells were videotaped for 20 min. The indicated time frames were processed using Adobe Photoshop software. Arrowheads point to protrusions. Bar is 10 μm.

surface (Figure 5C), suggesting that WIP$^{-/-}$ T cells may be unable to establish the sustained contact with the APC necessary for antigen-driven T cell activation.

Experiments with anti-CD3 on planar bilayers demonstrated that that CD3 is engaged and clustered in WIP$^{-/-}$ T cells similarly to WT T cells. Nevertheless, there was a profound defect in expansion of the contact area, which is a hallmark of early immunological synapse formation. Similar results were obtained with T cell-APC interactions triggered by SEA (Figure 6). LFA-1 clustering in the nascent immunological synapse was observed in response to antigen in WIP-deficient T cells, but the interface was not normal in that it never underwent the characteristic expansion observed for WT cells within 2 min of cell-cell contact. The finding that WIP$^{-/-}$ T cells can cluster LFA-1 in the interface suggests that LFA-1 activation may not require formation of new actin filaments and demonstrates that some actin-dependent functions, which also include actin cap formation, are intact in WIP$^{-/-}$ mice.

Electron microscopy revealed that the amount of F-actin associated with the cytoplasmic side of the adherent membrane was reduced in WIP $^{-/-}$ T cells and did not increase after CD3 ligation. Furthermore, actin filaments associated with adherent membranes were sparse, disrupted, and disorganized (Figure 7A). Disruption of the actin network is likely to explain the T cell defect in WIP$^{-/-}$ mice.

Crosslinking of the BCR has been reported to cause its translocation to lipid rafts and its association with the cytoskeleton in a detergent insoluble fraction (Braun et al., 1982; Cheng et al., 1999; Jugloff and Jongstra-Bilen, 1997). In spite of a reduced association of the actin cytoskeleton with the plasma membrane (Figure 7B), B cells from WIP$^{-/-}$ mice exhibited increased proliferation and CD69 expression in response to ligation of the BCR, anti-CD40, and LPS. This suggests that WIP and an intact actin cytoskeleton may be negative regulators of B cell activation. The opposite effect of WIP deficiency on the activation of T and B cells suggests that WIP and the actin network play fundamentally different roles in signaling by the TCR versus the BCR. While the TCR aggregates after stimulation, the BCR exists as an oligomer that is thought to dissociate following receptor ligation (Schamel and Reth, 2000). This dissociation may be inhibited by actin filaments. Since WIP stabilizes actin filaments, it may normally inhibit BCR signaling. Furthermore, while inhibition of actin polymerization by cytochalasin blocks raft assembly following TCR ligation, translocation of the BCR into rafts following crosslinking is not affected (Cheng et al., 2001), and B cell proliferation in response to BCR ligation is enhanced (Rothstein, 1985).

Some of the functions of WASP and its homolog N-WASP may be mediated by WIP. The ability of WASP to enhance TCR induction of NFAT activity and IL-2 expression depends on the WIP binding WH1 region of WASP (Silvin et al., 2001). It has been suggested that WASP/N-WASP and WIP function as a unit (Martinez-Quiles et al., 2001). This may explain the similarities between the phenotype of WIP$^{-/-}$ mice and that of WAS patients and WASP-deficient mice. WASP-deficient T cells proliferate poorly and fail to increase their F-actin content to anti-CD3. However, there are important differences be-

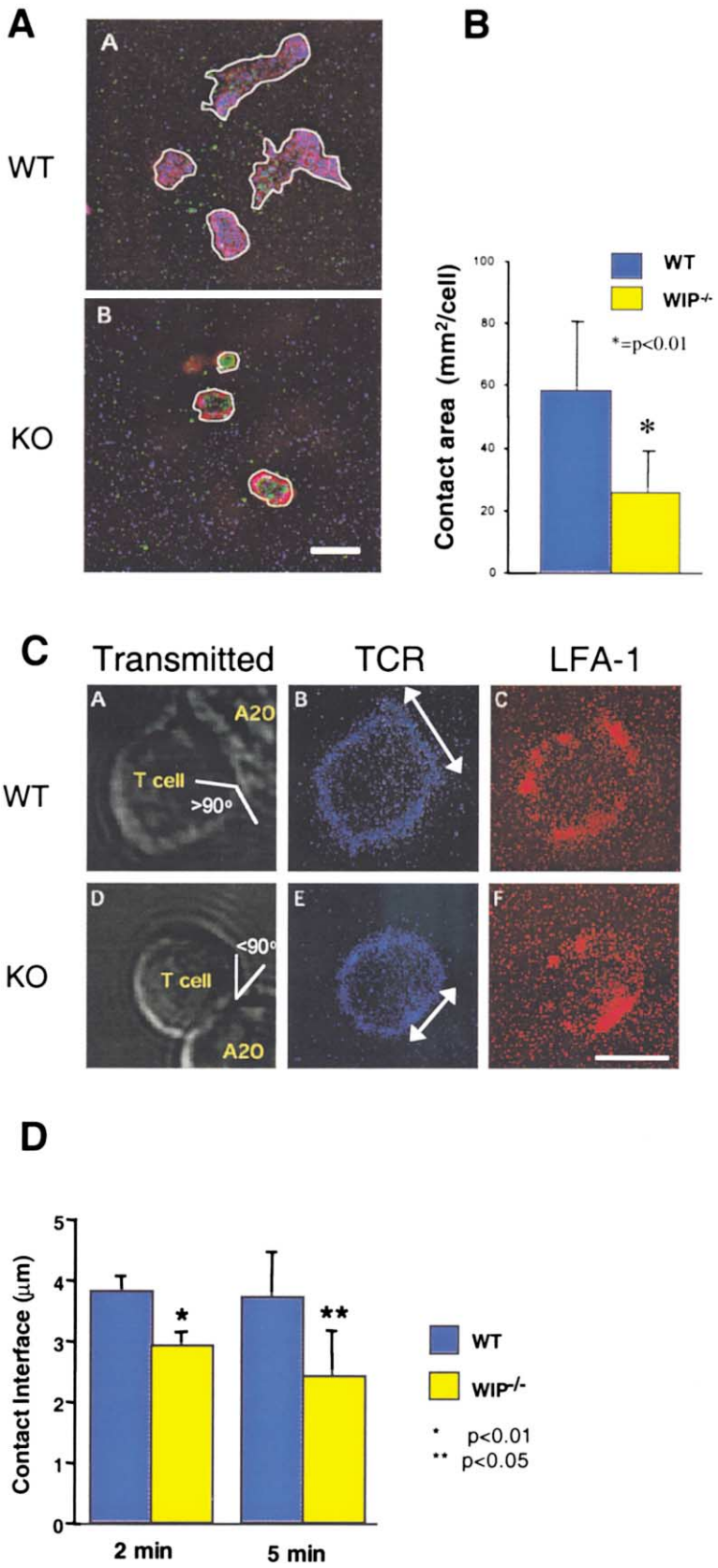

Figure 6. WIP$^{-/-}$ T Cells Cluster the TCR/CD3 Complex but Display a Significant Defect in Contact Area Expansion and Fail to Form an Expanded Interface with APC

(A) At 20 min, WT LN T cells interact with ICAM-1- and anti-CD3 FITC-containing bilayers (green). The cells were fixed and stained using phalloidin-rhodamine (for F-actin, red) and CtxB-cy5 (for GM1, blue). Therefore, purple indicates overlap of actin and cholera toxin. The CD3 antibody is laterally mobile in the bilayer, so accumulations of green indicate CD3-Ab interaction. The motility of WT cells results in some shedding of CD3 clusters that appear around the contact areas. Images were taken at the bilayer as determined by FITC brightness. Control bilayers lacking anti-CD3 showed no contact formation. At 20 min, WIP$^{-/-}$ lymph node T cells also interacted with the same type of bilayer and were fixed and stained as WT cells. The white outline indicates the contact area for each cell. Scale bar, 7 μm.

(B) Quantification of contact area with anti-CD3 bilayer based on two separate experiments. Statistical analysis used Student's t test with an n = 94.

(C) WIP$^{-/-}$ T cells polarize LFA-1 but fail to form an expanded interface with the APC. (A and D) Transmitted laser light image taken at 2 min of a lymph node T cell interacting with A20 B cell loaded with SEA (1 μM). (B and E) H57 Fab fragments labeled with Cy5 to mark the TCR. (C and F) H155 Fab fragments labeled with Cy3, marking LFA-1 fluorescence. The intersecting lines in (A) and (D) indicate the contact angle, which is greater than 90° for WT and less than 90° for the WIP$^{-/-}$. The arrows in (B) and (E) indicate the length of the contact interface. Scale bar, 4.5 μm.

(D) Analysis of length of contact interface at 2 and 5 min. T cell-A20 conjugates were measured at their widest interface, and averages were taken. Similar data were obtained in three separate experiments. Statistical analysis used Student's t test with an n = 31.

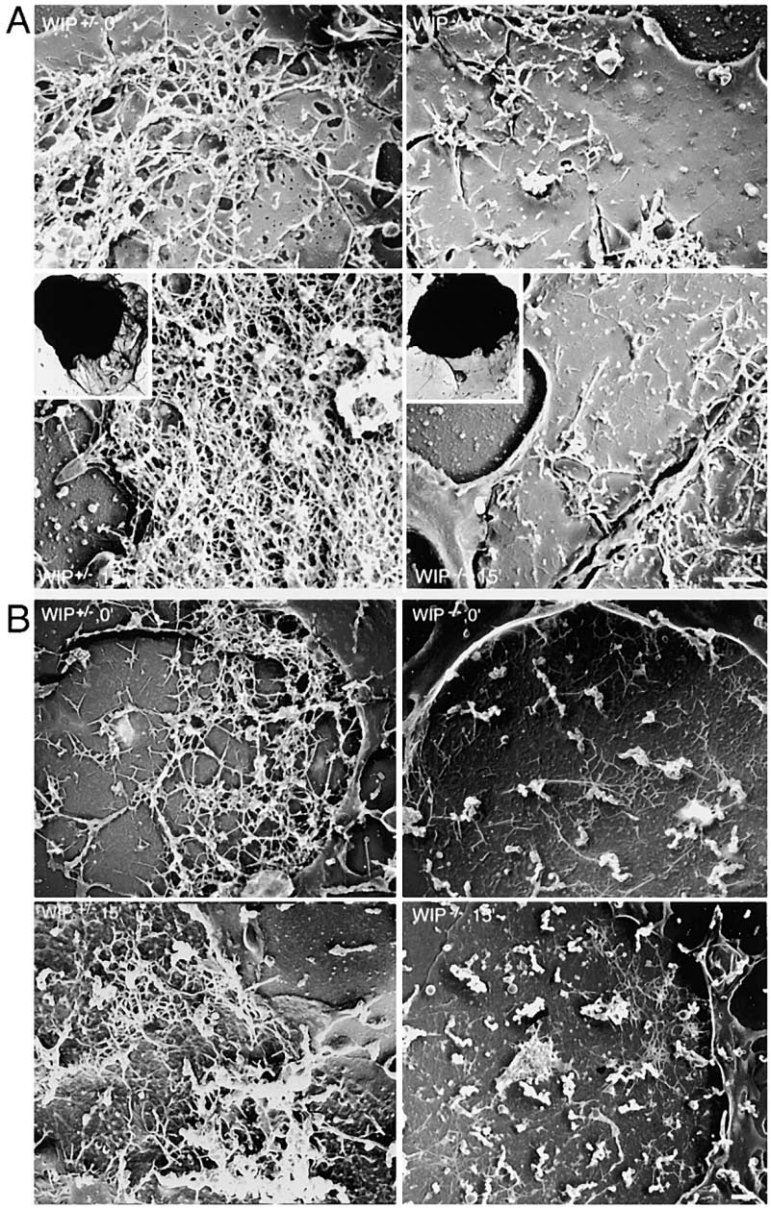

Figure 7. Subcortical Actin Network in WIP$^{-/-}$ T and B Lymphocytes

(A) Purified T lymphocytes from 8- to 10-week-old mice were adhered at 4°C to anti-CD3 coated coverslips and then allowed to spread for 0–15 min at 37°C. The cells were mechanically unroofed and cytoskeletal-membrane fragments prepared. Also, at the 15 min time point, intact cells were photographed. Left panels, WIP$^{+/-}$ T cells: (Upper panel) Organization of F-actin in a representative membrane fragment derived from an adhered but not spread cell at time zero. Actin filaments are present on the adherent membrane but in a less dense network than after 15 min of stimulation (see bottom panel). (Bottom panel) Organization of actin filaments within a protrusion made by a representative WIP$^{+/-}$ T cell after 15 min of incubation at 37°C. WIP$^{+/-}$ lymphocytes extend large blunt protrusions having convoluted surfaces. (Inset) Representative morphology of an intact WIP$^{+/-}$ lymphocyte allowed to spread for 15 min. Protrusions from WIP$^{+/-}$ cells are larger than those made by WIP$^{-/-}$ cells (compare to inset, right panel) and are filled with a dense matrix of F-actin. Right panels, WIP$^{-/-}$ T cells: (Upper panel) Adherent WIP$^{-/-}$ T cell at time zero. A sparse coat of actin filaments decorate the membrane. (Bottom panel) After 15 min of stimulation, the actin filament density in the membrane of the protrusions remain sparse and similar to that found in the adherent cell at time zero. (Inset) Activated WIP$^{-/-}$ lymphocytes only extend small protrusions. Bar is 200 nm.

(B) Purified B lymphocytes from 17-week-old mice were adhered at 4°C to anti-IgM coated coverslips, allowed to spread for 0–15 min at 37°C, and processed as above. Left panels, WIP$^{+/-}$ B cells: Unstimulated (upper panel) and stimulated (bottom panel) B cells show a similar density of actin filaments associated with the membrane. Right panels, WIP$^{-/-}$ B cells: Before (upper panel) and after stimulation (bottom panel), WIP-deficient B cells show sparse actin filaments associated with the membrane. Bar is 200 nm.

tween the functions of WIP and WASP. WASP/N-WASP enhance Arp2/3-dependent actin polymerization. In contrast, WIP diminishes N-WASP-mediated actin polymerization. Unlike WIP$^{-/-}$ mice, WASP$^{-/-}$ mice respond with a normal antibody response to TD antigens, and their B cells do not hyperproliferate in response to BCR ligation, anti-CD40, and LPS (Snapper et al., 1998; Zhang et al., 1999). Furthermore, the proliferative defect to anti-CD3 in WASP$^{-/-}$ T cells may be incomplete (Zhang et al., 1999) and is partially corrected by anti-CD28, whereas this defect is absolute in WIP$^{-/-}$ T cells and is not corrected by anti-CD28. This suggests that WASP and WIP can signal independently.

Our findings suggest a critical role for WIP in T cell activation and immune synapse formation, but not in B cell activation. Further studies are needed to define the exact link between the TCR and WIP.

Experimental Procedures

Generation of WIP-Deficient Mice

DNA encoding the murine *wip* gene was isolated by hybridizing a BAC library made from the 129/SvJ mouse strain (Genome Systems, Inc) with a fragment of mouse WIP cDNA. High-resolution restriction mapping yielded the genomic map of the *wip* gene. The targeting construct was assembled in the pLNTK targeting vector using a 4.5 kb EcoRI/XbaI blunted fragment and a 3.5 kb EcoRI/SacI blunted fragment. The construct (20 μg) was transfected by electroporation into ES cells (TC-1), which were then selected in medium containing 0.4 mg/ml of G418 and 10 μg/ml of gancyclovir. One of 97 clones found to contain both a normal and a disrupted allele and no random integration of the *neo* gene was injected into 3.5-day-old C57BL/6 blastocysts, and WIP$^{-/-}$ mice were obtained by standard methods (Tsitsikov et al., 1997).

Antibodies and Flow Cytometry Analysis

mAb mouse antigens were purchased from PharMingen and used for FACS as previously described (Hollander et al., 1996).

Serum Ig Levels and Antibody Responses to Antigen

Serum Ig levels were determined by ELISA (Tsitsikov et al., 1997). The antibody response to KLH, TNP-, and TNP-Ficoll was examined as previously described (Tsitsikov et al., 1997).

Proliferation of B and T Cells and Interleukin-2 Assay

Purified spleen B cells (>80% $B220^+$ cells) were cultured at 1×10^5/well in medium alone or in the presence of various stimuli and 48 hr later were pulsed with 1 μCi [^{3}H]-thymidine and counted.

Purified T cells (>95% $CD3^+$ cells) were cultured at 1×10^5/well for 64 hr in wells coated with 10 μg/ml anti-CD3 mAb (KT3, Serotec) with or without 10 μg/ml anti-CD28 mAb (37.51, BD Pharmingen). Recombinant murine IL-2 (R&D Systems) was used at 40 ng/ml. PMA was used at 15 ng/ml and ionomycin at 0.5 μM. Proliferation was assessed by the incorporation of [^{3}H]-thymidine. IL-2 in supernatants was measured by quantifying the proliferation of the IL-2-dependent cell line CTLL-2 (American Type Culture Collection) and by ELISA.

MAPK Kinase Assay

T cell activation was performed as previously described (Sun, 2000). Cell lysates were probed sequentially with anti-phospho-Erk, anti-Erk (both from SantaCruz Biotechnology), anti-phospho-SAPK/JNK, and anti-SAPK/JNK antibodies (Cell Signaling).

Determination of Cellular F-Actin

Purified T cells (4×10^6 cells/ml) were incubated with rat anti-mouse CD3 mAb (KT3, 10 μg/ml) for 30 min on ice, followed by crosslinking with goat anti-rat Ig (20 μg/ml) for 5 min at 37°C. They were then microspun, fixed in 4% formalin, washed, and permeabilized and stained in a single step with 0.1% Triton X-100 and 5 μg/ml Phalloidin-TRITC.

Fluorescence Microscopy and Time Lapse Videomicroscopy

Glass coverslips were coated with anti-CD3 mAb (KT3, 20 μg/ml in PBS) for 1 hr at 37°C and blocked with BSA. Purified T cells (1×10^6 cells/ml) were allowed to sediment on the coverslips for 30 min at 4°C. After washing off unattached cells, warm medium at 37°C was added, and cell movements were followed for 20 min on an IM-35 Zeiss microscope with a warm-stage. Images were acquired with an Orca-II cooled CCD camera driven by Metamorph software. Frames were taken every 5 s. After 20 min, the cells were fixed and stained for F-actin.

Lipid Bilayers

Purified lymph node T cells were loaded onto bilayers containing biotinylated 0.2% biotin-caproyl-phosphatidylethanolamine, egg lecithin, and Cy5-conjugated GPI-linked ICAM-1 (Pharmacia), ICAM-1 alone (control), or lecithin alone (control) in a flow cell chamber. Avidin-FITC (10 μg/ml) was added, and the bilayers were washed as described (Grakoui et al., 1999). Biotinylated anti-CD3ε (145-2C11, BD Biosciences, 10 μg/ml) was added and the bilayers washed. Cells at 37°C were added to the chamber at various times, fixed with 4% paraformaldehyde, and stained with CtxB-cy5 (Cholera Toxin B, Molecular Probes) and then with rhodamine phalloidin (10%, Molecular Probes). There were no interactions on the lecithin bilayer. Cells were imaged using a Zeiss LSM 510 confocal on an Axiovert 200 microscope. Analysis was performed using Zeiss LSM software. Backgrounds were subtracted, and averages and standard deviations were taken. Two-tailed t test was used to determine the statistical significance between WIP KO and WT counterparts in the same experiment.

T Cell-A20 B Lymphoma Cell Interactions

Purified splenic T cells were labeled at 4°C with Fab fragments of Cy5-labeled anti-TCR H57 mAb and Cy3-labeled anti-LFA-1 H155 mAb, then loaded at 37°C 3:1 onto A20 B lymphoma cells expressing I-E^kGFP (gift of M. Davis, Stanford University), and incubated at 37°C with medium or SEA superantigen (1 μM, Sigma). The cells were gently pelleted (200 rpm, 2 min), fixed with 4% paraformaldehyde, and imaged using a Zeiss LSM 510 confocal on an Axiovert 200 microscope. Analysis was performed using IP Lab. Statistical significances were determined using averages, standard deviations, and two-tailed t test.

Electron Microscopy

$WIP^{+/-}$ and $WIP^{-/-}$ T and B lymphocytes were allowed to adhere, respectively, to anti-CD3 coated and anti-IgM coated 5 mm glass coverslips. Coverslips were then warmed to 37°C for 0 or 15 min, then mechanically unroofed by attaching and removing a polylysine-coated coverslip to the apical cell surface after placing the cells in PHEM buffer (60 mM Pipes, 25 mM HEPES, 10 mM $MgCl_2$, and 10 mM EGTA) containing 1 μM phallacidin and protease inhibitors. Unroofed cells were washed once in PHEM buffer and fixed with 1% glutaraldehyde in PHEM buffer for 10 min. The coverslips were washed in distilled water, and cytoskeletons on the surface were frozen by slamming them into a liquid helium-cooled copper block. Some coverslips were fixed without unroofing in 1% glutaraldehyde in PBS. All specimens were freeze-dried in a Cressington CFE-50 apparatus (Cressington, Watford, England) at −90°C and rotary coated with 1.4 nm of platinum and 3.0 nm of carbon without rotation. They were photographed in a JEOL 1200 EX electron microscope using a 100 kV accelerating voltage.

Acknowledgments

We thank Mike Byrne and Karin Horney for technical assistance; Dr. Paul Bryce for statistical analysis; and Drs. Ignacio Moreno de Alborán, Scott Snapper, and Fred Alt for useful discussions and valuable reagents. I.M.A. is a recipient of a Lady Tata Memorial Trust Award, and M.A.F. is supported by a Spanish Ministry of Science and Technology postdoctoral grant (EX 99 12368513).

This work was supported by USPHS grants 59561 and by grants from Baxter, Aventis, and Gentiva Corporations; the Jeffrey Model Foundation; and the March of Dimes.

Received June 13, 2001, revised November 30, 2001.

References

Acuto, O., and Cantrell, D. (2000). T cell activation and the cytoskeleton. Annu. Rev. Immunol. *18*, 165–184.

Aspenstrom, P., Lindberg, U., and Hall, A. (1996). Two GTPases, Cdc42 and Rac, bind directly to a protein implicated in the immunodeficiency disorder Wiskott-Aldrich syndrome. Curr. Biol. *6*, 70–75.

Benschop, R.J., and Cambier, J.C. (1999). B cell development: signal transduction by antigen receptors and their surrogates. Curr. Opin. Immunol. *11*, 143–151.

Braun, J., Hochman, P.S., and Unanue, E.R. (1982). Ligand-induced association of surface immunoglobulin with the detergent-insoluble cytoskeletal matrix of the B lymphocyte. J. Immunol. *128*, 1198–1204.

Bunnell, S.C., Kapoor, V., Trible, R.P., Zhang, W., and Samelson, L.E. (2001). Dynamic actin polymerization drives T cell receptor-induced spreading a role for the signal transduction adaptor LAT. Immunity *14*, 315–329.

Cheng, P.C., Dykstra, M.L., Mitchell, R.N., and Pierce, S.K. (1999). A role for lipid rafts in B cell antigen receptor signaling and antigen targeting. J. Exp. Med. *190*, 1549–1560.

Cheng, P.C., Brown, B.K., Song, W., and Pierce, S.K. (2001). Translocation of the B cell antigen receptor into lipid rafts reveals a novel step in signaling. J. Immunol. *166*, 3693–3701.

Derry, J.M.J., Ochs, H.D., and Francke, U. (1994). Isolation of a novel gene mutated in Wiskott-Aldrich syndrome. Cell *78*, 635–644.

Dustin, M.L., and Cooper, J.A. (2000). The immunological synapse and the actin cytoskeleton: molecular hardware for T cell signaling. Nat. Immunol. *1*, 23–29.

Gallego, M.D., Santamaria, M., Pena, J., and Molina, I.J. (1997). Defective actin reorganization and polymerization of Wiskott-Aldrich T cells in response to CD3-mediated stimulation. Blood *90*, 3089–3097.

Grakoui, A., Bromley, S.K., Sumen, C., Davis, M.M., Shaw, A.S., Allen, P.M., and Dustin, M.L. (1999). The immunological synapse: a

molecular machine controlling T cell activation. Science *285*, 221–227.

Hollander, G., Castigli, E., Kulback, R., Su, M., Burakoff, S., Gutierrez-Ramos, J.-C., and Geha, R. (1996). Induction of alloantigen-specific tolerance by B cells fron CD40 deficient mice. Proc. Natl. Acad. Sci. USA *93*, 4994–4998.

Holsinger, L.J., Graef, I.A., Swat, W., Chi, T., Bautista, D.M., Davidson, L., Lewis, R.S., Alt, F.W., and Crabtree, G.R. (1998). Defects in actin-cap formation in vav-deficient mice implicate an actin requirement for lymphocyte signal transduction. Curr. Biol. *8*, 563–572.

Jugloff, L.S., and Jongstra-Bilen, J. (1997). Cross-linking of the IgM receptor induces rapid translocation of IgM-associated Ig alpha, Lyn, and Syk tyrosine kinases to the membrane skeleton. J. Immunol. *159*, 1096–1106.

Kim, A.S., Kakalis, L.T., Abdul-Manan, N., Liu, G.A., and Rosen, M.K. (2000). Autoinhibition and activation mechanisms of the Wiskott-Aldrich syndrome protein. Nature *404*, 151–158.

Klasen, S., Pages, F., Peyron, J.F., Cantrell, D.A., and Olive, D. (1998). Two distinct regions of the CD28 intracytoplasmic domain are involved in the tyrosine phosphorylation of Vav and GTPase activating protein-associated p62 protein. Int. Immunol. *10*, 481–489.

Kolluri, R., Tolias, K.F., Carpenter, C.L., Rosen, F.S., and Kirchhausen, T. (1996). Direct interaction of the Wiskott-Aldrich syndrome protein with GTPase Cdc42. Proc. Natl. Acad. Sci. USA *93*, 5615–5618.

Krause, M., Sechi, A.S., Konradt, M., Monner, D., Gertler, F.B., and Wehland, J. (2000). Fyn-binding protein (Fyb)/SLP-76-associated protein (SLAP), Ena/vasodilator-stimulated phosphoprotein (VASP) proteins and the Arp2/3 complex link T cell receptor (TCR) signaling to the actin cytoskeleton. J. Cell Biol. *149*, 181–194.

Kurosaki, T., Maeda, A., Ishiai, M., Hashimoto, A., Inabe, K., and Takata, M. (2000). Regulation of the phospholipase C-gamma2 pathway in B cells. Immunol. Rev. *176*, 19–29.

Machesky, L., and Insall, R. (1998). Scar1 and the related Wiskott-Aldrich syndrome protein, WASP, regulate the actin cytoskeleton through the Arp2/3 complex. Curr. Biol. *8*, 1347–1356.

Martinez-Quiles, N., Rohatgi, R., Anton, I.M., Medina, M., Saville, S.P., Miki, H., Yamaguchi, H., Takenawa, T., Hartwing, J., Geha, R.S., and Ramesh, N. (2001). WIP regulates N-WASP mediate actin polymerization and filopodium formation. Nat. Cell Biol. *3*, 484–491.

Miki, H., Miura, K., and Takenawa, T. (1996). N-WASP, a novel actin-depolymerizing protein, regulates the cortical cytoskeletal rearrangement in a PIP2-dependent manner downstream of tyrosine kinases. EMBO J. *15*, 5326–5335.

Miki, H., Suetsugu, S., and Takenawa, T. (1998a). WAVE, a novel WASP-family protein involved in actin reorganization induced by Rac. EMBO J. *17*, 6932–6941.

Miki, H., Sasaki, T., Takai, Y., and Takenawa, T. (1998b). Induction of filopodium formation by a WASP-related actin-depolymerizing protein N-WASP. Nature *391*, 93–96.

Molina, I.J., Sancho, J., Terhorst, C., Rosen, F.S., and Remold-O'Donnell, E. (1993). T cells of patients with the Wiskott-Aldrich syndrome have a restricted defect in proliferative responses. J. Immunol. *151*, 4383–4390.

Monks, C.R., Freiberg, B.A., Kupfer, H., Sciaky, N., and Kupfer, A. (1998). Three-dimensional segregation of supramolecular activation clusters in T cells. Nature *395*, 82–86.

Moreau, V., Frischknecht, F., Reckmann, I., Vincentelli, R., Rabut, G., Stewart, D., and Way, M. (2000). A complex of N-WASP and WIP integrates signalling cascades that lead to actin polymerization. Nat. Cell Biol. *2*, 441–448.

Negulescu, P.A., Krasieva, T.B., Khan, A., Kerschbaum, H.H., and Cahalan, M.D. (1996). Polarity of T cell shape, motility, and sensitivity to antigen. Immunity *4*, 421–430.

Parsey, M.V., and Lewis, G.K. (1993). Actin polymerization and pseudopod reorganization accompany anti-CD3-induced growth arrest in Jurkat cells. J. Immunol. *151*, 1881–1893.

Penninger, J.M., and Crabtree, G.R. (1999). The actin cytoskeleton and lymphocyte activation. Cell *96*, 9–12.

Phatak, P.D., and Packman, C.H. (1994). Engagement of the T-cell antigen receptor by anti-CD3 monoclonal antobody causes a rapid increase in lymphocyte F-actin. J. Cell. Physiol. *159*, 365–370.

Ramesh, N., Anton, I.M., Hartwig, J.H., and Geha, R.S. (1997). WIP, a protein associated with the Wiskott-Aldrich Syndrome Protein, induces actin polymerization and redistribution in lymphoid cells. Proc. Natl. Acad. Sci. USA *94*, 14671–14676.

Risso, A., Cosulich, M.E., Rubartelli, A., Mazza, M.R., and Bargellesi, A. (1989). MLR3 molecule is an activation antigen shared by human B, T lymphocytes and T cell precursors. Eur. J. Immunol. *19*, 323–328.

Rohatgi, R., Ho, H.H., and Kirschner, M.W. (2000). Mechanism of N-WASP activation by Cdc42 and Phosphatidylinositol 4,5-bisphosphate. J. Cell Biol. *150*, 1299–1309.

Rothstein, T.L. (1985). Anti-immunoglobulin in combination with cytochalasin stimulates proliferation of murine B lymphocytes. J. Immunol. *135*, 106–110.

Rozdzial, M.M., Malissen, B., and Finkel, T.H. (1995). Tyrosine-phosphorylated T cell receptor zeta chain associates with the actin cytoskeleton upon activation of mature T lymphocytes. Immunity *3*, 623–633.

Rudd, C.E. (1996). Upstream-downstream: CD28 cosignaling pathways and T cell function. Immunity *4*, 527–534.

Savoy, D.N., Billadeau, D.D., and Leibson, P.J. (2000). Cutting edge: WIP, a binding partner for Wiskott-Aldrich syndrome protein, cooperates with Vav in the regulation of T cell activation. J. Immunol. *164*, 2866–2870.

Schamel, W.W., and Reth, M. (2000). Monomeric and oligomeric complexes of the B cell antigen receptor. Immunity *13*, 5–14.

Silvin, C., Belisle, B., and Abo, A. (2001). A role for WASP in TCR-mediated transcriptional activation independent of actin polymerization. J. Biol. Chem. *276*, 21450–21457.

Snapper, S.B., Rosen, F.S., Mizoguchi, E., Cohen, P., Khan, W., Liu, C.-H., Hagemann, T.L., Kwan, S.-P., Ferrini, R., Davidson, L., et al. (1998). Wiskott-Aldrich Syndrome protein-deficient mice reveal a role for WASP in T but not B cell activation. Immunity *9*, 81–91.

Sun, Z., Arendt, C.W., Ellmeier, W., Schaeffer, E.M., Sunshine, M.J., Gandhi, L., Annes, J., Petrzilka, D., Kupfer, A., Schwartzberg, P.L., and Littman, D.R. (2000). PKC-θ is required for TCR-induced NF-κB activation in mature but not immature T lymphocytes. Nature *404*, 402–407.

Symons, M., Derry, J.M.J., Kariak, B., Jiang, S., Lemahieu, V., McCormick, F., Francke, U., and Abo, A. (1996). Wiskott-Aldrich syndrome protein, a novel effector for the GTPase Cdc42Hs, is implicatd in actin polymerization. Cell *84*, 723–734.

Tsitsikov, E.N., Gutierrez-Ramos, J.C., and Geha, R.S. (1997). Impaired CD19 expression and signaling, enhanced antibody response to type II T independent antigen and reduction of B-1 cells in CD81-deficient mice. Proc. Natl. Acad. Sci. USA *94*, 10844–10849.

Vaduva, G., Martinez-Quiles, N., Anton, I.M., Martin, N.C., Geha, R.S., Hopper, A.K., and Ramesh, N. (1999). The human WASP-interacting Protein, WIP, activates the cell polarity pathway in yeast. J. Biol. Chem. *274*, 17103–17108.

Valitutti, S., Dessing, M., Aktories, K., Gallati, H., and Lanzavecchia, A. (1995). Sustained signaling leading to T cell activation results from prolonged T cell receptor occupancy. Role of T cell actin cytoskeleton. J. Exp. Med. *181*, 577–584.

Wulfing, C., Sjaastad, M.D., and Davis, M.M. (1998). Visualizing the dynamics of T cell activation: intracellular adhesion molecule 1 migrates rapidly to the T cell/B cell interface and acts to sustain calcium levels. Proc. Natl. Acad. Sci. USA *95*, 6302–6307.

Wulfing, C., Bauch, A., Crabtree, G.R., and Davis, M.M. (2000). The vav exchange factor is an essential regulator in actin-dependent receptor translocation to the lymphocyte-antigen-presenting cell interface. Proc. Natl. Acad. Sci. USA *97*, 10150–10155.

Zhang, J., Shehabeldin, A., da Cruz, L.A., Butler, J., Somani, A.K., McGavin, M., Kozieradzki, I., dos Santos, A.O., Nagy, A., Grinstein, S., et al. (1999). Antigen receptor-induced activation and cytoskeletal rearrangement are impaired in Wiskott-Aldrich syndrome protein-deficient lymphocytes. J. Exp. Med. *190*, 1329–1342.